

## A MICROFABRICATED ULTRASONIC PARTICLE MANIPULATOR WITH FREQUENCY SELECTABLE NODAL PLANES

**M. Hill<sup>+</sup>, N.R. Harris<sup>#</sup>, R.J. Townsend<sup>+</sup>, N.M. White<sup>#</sup>, and S.P. Beeby<sup>#</sup>**

<sup>+</sup>School of Engineering Sciences, Southampton University, Southampton, UK

<sup>#</sup> Electronics and Computer Science, Southampton University, Southampton, UK

m.hill@soton.ac.uk

### Abstract

Ultrasonic devices designed to manipulate particles rely on an ability to predict the nature of the standing wave within a resonator. The interaction between the properties of the layers within the resonator can generate standing waves that vary significantly from the classic rigid boundary model for half-wavelength resonances.

A simple, two layer, model demonstrates the dependence of standing wave characteristics on the impedance of a reflecting boundary. A multi-layer model that includes a representation of the primary radiation forces on particles is then used to refine the resonator design and allow for interactions with the other layers.

Both models predict that resonators with sub-wavelength critical dimensions can be designed with multiple modes each with pressure nodes at different positions. The models have been used to design a microfabricated resonator with modes that allow particles to be forced to either boundary of the fluid or to the fluid centre, depending on the operating frequency.

### Introduction

Ultrasonic standing waves generate small forces on particles within the acoustic field which tend to move those particles to the pressure nodes or antinodes [1, 2] of the field. Design of resonators to manipulate particles demands a model of the acoustic field and the radiation forces generated within it. Several models of the acoustic radiation forces within standing waves have been developed[3-5] and these have typically been used to provide analytical solutions for the force profiles within idealised standing waves.

The electro-acoustic characteristics of more general planar standing waves have been modelled successfully as layered resonators [1, 6-9]. This paper uses two models of standing wave characteristics to examine how the thickness of the reflector and fluid layers can be chosen to determine the position of the pressure nodal plane within the fluid layer.

### Theory

A layered resonator, such as those typically used for ultrasonic particle manipulation is shown diagrammatically in Figure 1.

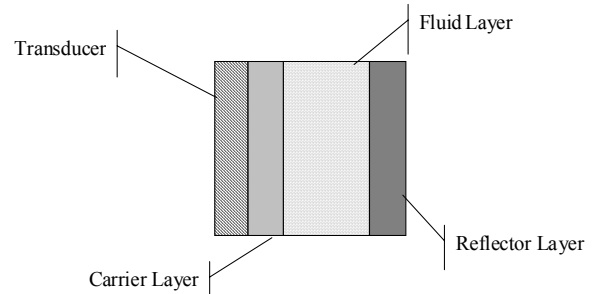


Figure 1: A typical structure for a fluid resonator

The nature of the acoustic standing wave generated within the fluid layer will be a function of the transducer's driving frequency and amplitude, but also of the acoustic impedances presented to each of the layers. To isolate the nature of the standing wave's dependence on the relative impedance of the fluid layer and the reflector layer, consider a simplified resonator in which the left hand boundary of the fluid layer is driven by a constant amplitude sinusoidal displacement. It can be shown that acoustic modes representing energy maxima in the fluid layer will occur when[10]:

$$k_f t_f = \tan^{-1} \left( \frac{r_f (r_r^2 + r_0^2 \tan^2(k_r t_r))}{r_r \tan(k_r t_r) (r_r^2 - r_0^2)} \right) \quad (1)$$

where  $k$  is a wave number,  $t$  a thickness and  $r$  a characteristic acoustic impedance. Subscripts  $f$  and  $r$  denote the fluid and reflector properties respectively and  $r_0$  is the impedance at the termination of the reflector layer.

Table 1: Material properties used in simulations

Layer	Material	Density (kgm <sup>-3</sup> )	Speed of Sound (ms <sup>-1</sup> )
Fluid	water	1000	1500
Reflector	Pyrex	2200	5430
Reflector	air	1.3	330
Termination			

For a given set of impedance values, a graph showing solutions to this equation such as that shown in Figure 2 can be generated. The values used in this graph are for an example water filled resonator with a Pyrex reflector and the values used are shown in Table 1. For a particular resonator design the values of  $t_f/c_f$  and  $t_r/c_r$  may be assumed to be constant, so a "frequency sweep" is represented on the graph by a

straight line passing through zero, of gradient  $t_f c_r / t_r c_f$ .

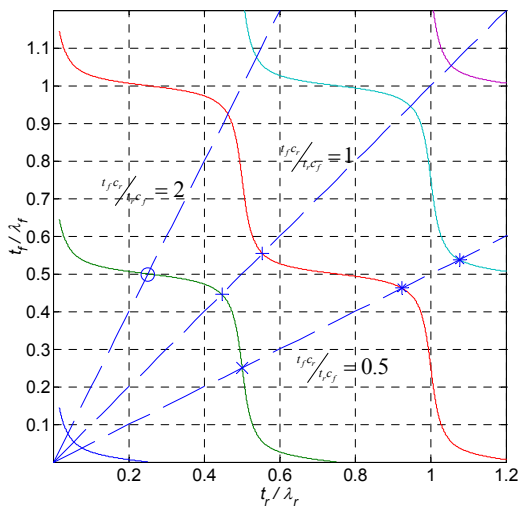


Figure 2: The first four solutions to equation (1).

Three such “frequency sweeps” are shown as dotted lines over the solutions to equation (1). These three represent resonators in which  $t_f c_r / t_r c_f$  is equal to 2, 1, and 0.5. In the first case, the resonance marked by a “o” is a half wavelength mode, in which, at the modal frequency, the fluid layer is half the wavelength in thickness and the reflector layer is a quarter wavelength in thickness. The next “frequency sweep” has two resonances marked by a “+”. These are near half wavelengths in both fluid and reflector waves and are similar to the coupled resonator case described by Hawkes *et al.* [7, 9].

The final “frequency sweep”, for a resonator in which  $t_f c_r / t_r c_f = 0.5$ , has a resonance marked by an “x”. At the frequency of this mode the fluid layer is a quarter wavelength thick and the reflector layer is a half wavelength thick. For this resonator at this frequency the primary acoustic radiation force will move particles within the fluid to the boundary with the reflector, as in contrast to the case with a perfectly rigid boundary, the half wave resonance in the reflector layer causes the pressure node to be up against the solid boundary itself. Also of note for this resonator geometry are the two higher frequency modes marked with a “\*”. These modes occur at frequencies which are either side of a half wavelength in the fluid layer. The existence of both quarter wave and near half wavelength modes in the same geometry resonator suggests that it should be possible to build a resonator with modes which will move particles to either the centre of the fluid layer or to the fluid/resonator boundary, depending on the driving frequency selected.

**Design of an experimental system**

In order to demonstrate the existence of a resonator with multiple resonances capable of moving particles to either the centre of the boundary of a fluid a fuller simulation was required which modelled all the layers in the resonator, not just the fluid and reflector layers. The fuller simulation is needed as, just as the fluid and reflector layers interact, so the other layers in the resonator will influence the position and nature of an acoustic mode in the fluid layer.

*Numerical multi-layer model predictions*

The model used is that described by Hill *et al.* [8, 9]. The structure of the resonator was based on that previously described by Harris *et al.* [11] and consists of a 3 MHz thickness mode PZT transducer glued to a 525 μm thick silicon carrier layer. The carrier layer is anodically bonded to a Pyrex layer into which the fluid cavity has been etched. Hence the material properties are fixed but the cavity thickness (and the associated reflector thickness) becomes the primary design variable. The Pyrex wafer used is 1.7 mm thick, so as the fluid cavity is etched into this, the sum of the fluid and reflector thicknesses will be 1.7 mm. Given the material properties in layer 1 and this constraint on total fluid/reflector thickness, the condition  $t_f c_r / t_r c_f = 0.5$  will be met when  $t_f$  is about 200 μm and  $t_r$  1500 μm. Such a fluid layer depth would correspond to a quarter wave resonance of about 1.8 MHz. This was used as the basis for a simulation of the variation of energy density within the fluid layer as a function of frequency and etch depth as shown in Figure 3.

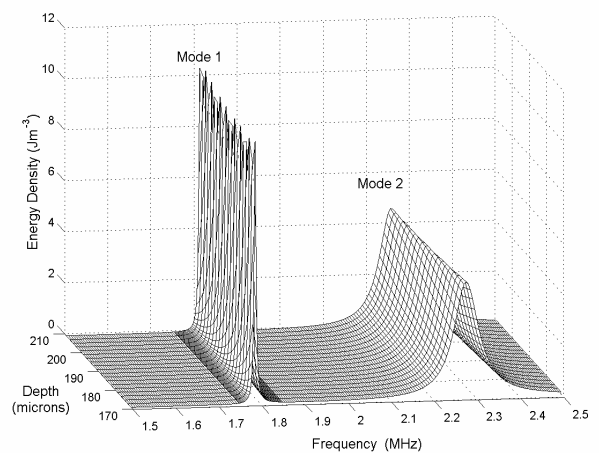


Figure 3: Energy density against fluid layer depth and frequency between 1.5 & 2.5 MHz

The predicted quarter wave mode, marked with an “x” in Figure 2 corresponds to “mode 1” in Figure 3. The predicted near half-wavelength modes marked with “\*” symbols in Figure 2 can be seen in Figure 4, which displays the same plot as Figure 3 but over a higher frequency range.

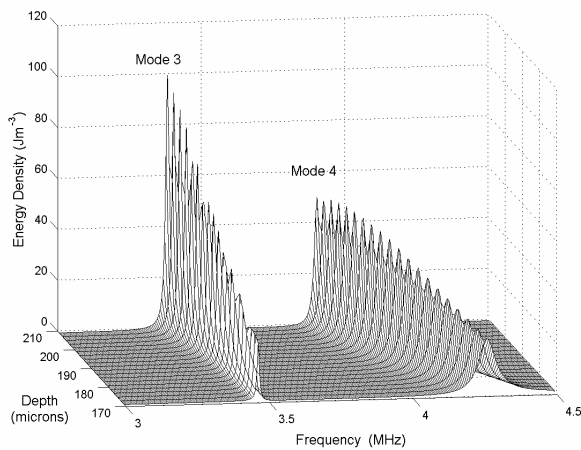


Figure 4: As Figure 3 for frequencies, between 3 & 4.5 MHz. Note different energy density scale.

The energy peak marked as “mode 2” in Figure 3 is not predicted by Figure 2, however. To confirm the nature of modes 1, 3 & 4, and to investigate the nature of mode 2, predictions of the pressure amplitude across the fluid layer (and its variation with fluid layer depth) can be plotted, as in Figure 5

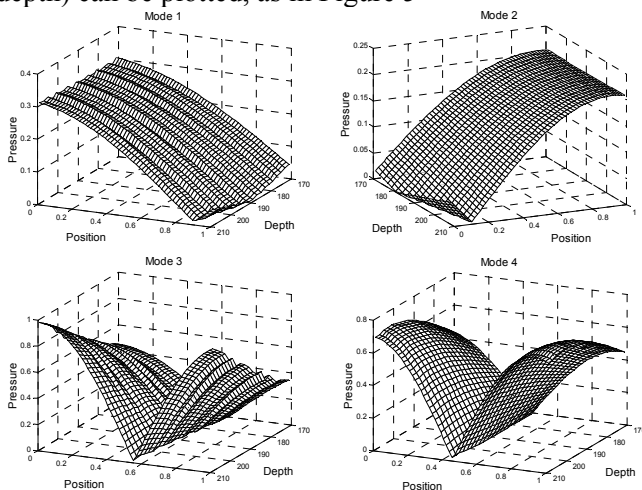


Figure 5: Modelled fluid layer pressure distributions against fractional distance from the carrier layer for the four modes against etched cavity depth (microns).

As expected, mode 1 has a maximum pressure at the carrier layer boundary and a pressure minimum at or near the reflector boundary. Modes 3&4 are similar to typical half wave (rigid-rigid boundary) modes with a pressure minimum near the centre of the cavity. It is now apparent that mode 2 is also a quarter wave mode, but with its pressure minimum at the carrier layer boundary and a maximum at the reflector. This mode appears due to a resonance within the carrier layer and hence was not predicted by the analytical model used to generate Figure 2

### Experimental Results

The model described above suggests that, over the frequency range of interest, two quarter and two half

wavelength modes should be generated for any of the cavity depths modelled between 170 and 210  $\mu\text{m}$ . However a close look at modes 1 & 2 in Figure 5 shows that the model predicts the pressure nodes to be slightly away from the respective boundaries at the higher end of the cavity depth range. Hence a value of 175  $\mu\text{m}$  was chosen for the etch depth.

### Impedance Characteristics

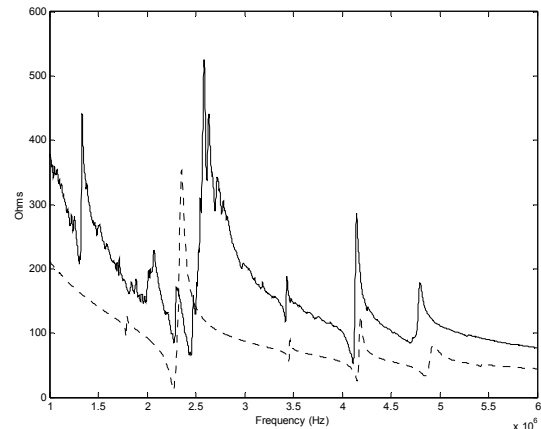


Figure 6: Modelled (dotted) and measured (solid) impedance plots for the fluid filled device

Figure 6 shows the input impedance to the resonator as predicted by the multi-layer model and the measured input impedance. Impedance peaks due to modes 3&4 are clearly visible at about 3.5 and 4.1 MHz in both modelled and measured results. However the model is a simplification of the actual resonator, and in particular only considers behaviour in a single dimension, making the measured results more complex than the modelled results at frequencies below about 3 MHz. A small impedance peak in the modelled results at 1.8 MHz corresponds to mode 1, but is not clearly distinguishable in the measured results. Mode 2 is completely masked by the large transducer/carrier layer peak visible at about 2.4 MHz in the modelled and 2.7 MHz in the measured results.

### Particle Manipulation

An optical microscope, focussed through the Pyrex reflector layer was used to monitor the position of yeast particles within the fluid layer of the resonator. The device was driven from a frequency synthesiser, via a fixed gain RF amplifier (50dB). The transducer was placed in series with a 47ohm resistance to allow the variation in voltage across the transducer to be monitored to identify voltage minima. This proved a more sensitive means of identifying modes than the impedance sweep of Figure 6. By searching for voltage minima in the region predicted by the model, all four modes were identified. Modes were found at 1.71MHz, 2.27MHz, 3.44MHz and 4.1MHz,

although, modes 1 and 2 required very careful adjustment to identify.

The position of the particles within the fluid layer was monitored by using the small depth of field of the microscope. For example, in the case of mode 1, the microscope was focussed on the boundary between the fluid and the reflector layers.

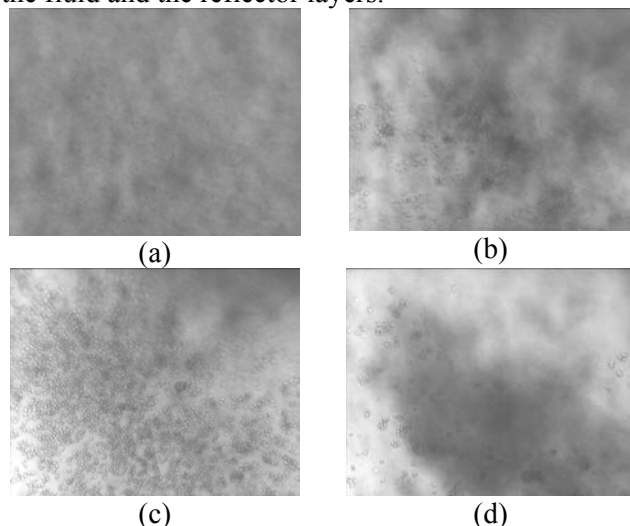


Figure 7: A sequence of images taken as particles move to the reflector boundary driven at the frequency of mode 1.

Figure 7 shows randomly distributed particles being forced to the Pyrex/water boundary against gravity as predicted for Mode 1 at 1.7MHz. Image (a) shows the random distribution of yeast before any power is applied, with the microscope focussed at the Pyrex/water boundary. Image (b) shows the view 5 seconds after the power is applied, and it can be seen that yeast cells are beginning to move into focus as they are forced against the boundary. Image (c) shows the situation after 15 seconds and many more cells are now in focus. Particles tend to collect in clumps due to lateral forces, and image (d), taken 40 seconds later, after the power has been turned off shows this. The clump of particles is peeling away from the Pyrex layer and falling under the influence of gravity towards the silicon layer and thus out of focus.

Similar results were obtained for the other three modes, showing that particles could be forced to either of the cavity boundaries or to the cavity centre.

### Conclusions

A simple analytical equation which predicts the combination of thicknesses of two layers required to produce an acoustic mode with a specifically positioned pressure node has been used in the initial design of a resonator with both quarter and half wavelength modes. The modelling has been further refined using a simulation of a full resonator system.

A device has been built using microfabrication techniques and has been shown to be able to move particles to either boundary of the fluid layer or to the

centre of the fluid layer, depending on the driving frequency (and hence the particular mode).

Although the quarter wave modes were more difficult to identify and drive, such a system offers the potential to move cells or particles within a fluid in a controlled manner.

### Acknowledgements

This work has been carried out with financial support from Dstl and EPSRC under grant number GR/R13333/01, and Porvair PLC.

### References

- [1] M. Gröschl, "Ultrasonic separation of suspended particles - Part I: Fundamentals," *Acustica*, vol. 84, pp. 432-447, 1998.
- [2] W. T. Coakley, "Ultrasonic separations in analytical biotechnology," *Trends in Biotechnology*, vol. 15, pp. 506-511, 1997.
- [3] L. V. King, "On the acoustic radiation pressure on spheres," *Proc R. Soc. London*, vol. A147, pp. 212-40, 1934.
- [4] K. Yosioka and Y. Kawasima, "Acoustic radiation pressure on a compressible sphere," *Acustica*, vol. 5, pp. 167-73, 1955.
- [5] S. D. Danilov and M. A. Mironov, "Radiation pressure force acting on a small particle in a sound field.," *Sov. Phys. Acoust.*, vol. 30, pp. 280-3, 1984.
- [6] H. Nowotny and E. Benes, "General One-Dimensional Treatment of the Layered Piezoelectric Resonator with 2 Electrodes," *Journal of the Acoustical Society of America*, vol. 82, pp. 513-521, 1987.
- [7] J. J. Hawkes, M. Gröschl, H. Nowotny, S. Armstrong, P. Tasker, W. T. Coakley, and E. Benes, "Single half wavelength ultrasonic particle filter: Predictions of the transfer matrix multi-layer resonator model and experimental filtration results.," *Journal of the Acoustical Society of America*, vol. 111, pp. 1259-1266, 2002.
- [8] M. Hill and R. J. K. Wood, "Modelling in the design of a flow-through ultrasonic separator," *Ultrasonics*, vol. 38, pp. 662-665, 2000.
- [9] M. Hill, Y. Shen, and J. J. Hawkes, "Modelling of layered resonators for ultrasonic separation.," *Ultrasonics*, vol. 40, pp. 385-92, 2002.
- [10] M. Hill, "The selection of layer thicknesses to control acoustic radiation force profiles in layered resonators," *JASA. In press.*
- [11] N. R. Harris, M. Hill, S. P. Beeby, Y. Shen, N. M. White, J. J. Hawkes, and W. T. Coakley, "A Silicon Microfluidic Ultrasonic Separator," *Sensors and Actuators B*, vol. 95, pp. 425-34, 2003.